

The use of angle resolved XPS to measure the fractional coverage of high-*k* dielectric materials on silicon and silicon dioxide surfaces

P. Mack^a, R.G. White^a, J. Wolstenholme^{a,*}, T. Conard^b

^a Thermo Electron, Imberhorne Lane, East Grinstead, West Sussex, RH19 1UB, UK

^b IMEC, Kapeldreef 75, B-3001, Leuven, Belgium

Received 9 September 2005; received in revised form 25 September 2005; accepted 29 October 2005

Available online 2 December 2005

Abstract

Angle resolved XPS (ARXPS) is a powerful tool for the determination of the thickness of ultra-thin films. In the case of high-*k* dielectric layers, the technique is capable of measuring the thickness of both the high-*k* layer and intermediate layers of silicon dioxide or metal silicate. The values for layer thickness are in close agreement with those generated by a variety of other techniques. As well as knowing the thickness of these layers, it is important to determine whether the layers are continuous or whether the coverage of the high-*k* layer is only partial. Using ARXPS, a method has been developed to determine whether the coverage of the high-*k* material is continuous and, if not, to calculate the fraction of the surface that is covered. The method is described with reference to the layers of Al₂O₃ grown on SiO₂ using atomic layer deposition (ALD). The method is then applied to HfO₂ layers produced using ALD on silicon wafers whose surfaces had received three different types of surface treatment. The way in which the layers grow and the nature of the resulting layer were found to depend upon the pre-treatment method. For example, growth on a thermal silicon dioxide surface resulted in complete coverage of HfO₂ after fewer ALD cycles than layers grown on an H-terminated surface. The results from ARXPS are compared with those obtained from ToF SIMS that have been shown earlier to be a valuable alternative to the LEIS analysis [1].
© 2005 Elsevier B.V. All rights reserved.

Keywords: Angle resolved XPS; High-*k* dielectric; Hafnium oxide; Aluminium oxide; Island growth

1. Introduction

Angle resolved XPS (ARXPS) has been shown to be a powerful tool for the determination of the thickness of ultra-thin films. With careful choice of constants, the method can be applied with accuracy and precision [2]. The method is based upon a model that assumes that an XPS signal is attenuated as it passes through a material according to an expression similar to that used in other forms of spectroscopy, the Beer–Lambert expression:

$$I = I_0 \exp(-d/\lambda)$$

According to this equation, an XPS signal having intensity I_0 will be attenuated to intensity, I , after travelling a distance, d , in

the material. The constant, λ , is known as the attenuation length.

Similarly, the XPS signal from a bulk material, following attenuation by a thin layer of some other material at its surface (e.g. the signal from a metal having a thin native oxide at its surface) can be calculated. The signal from the bulk material detected at the surface, at some angle, θ , to the surface normal, is given by

$$I = I_0 \exp(-d/\lambda \cos \theta) \quad (1)$$

This equation can be manipulated to allow the measurement of layer thickness provided that the layers are less than about 3λ . In order to do this, of course, it is essential that the value of λ be known for the material in question at the kinetic energy of the electrons providing the signal. For many materials, the value of this quantity can be found in the literature. Alternatively it can be calculated using a two-step process. First, the inelastic mean free path, IMFP, is calculated using the TPP-2M equation of

* Corresponding author. Tel.: +44 1342 327211; fax: +44 1342 324613.
E-mail address: john.wolstenholme@thermo.com (J. Wolstenholme).

Tanuma et al. [3] (this is the same equation as that used in the 'NIST Electron Effective Attenuation Length Database [4]). In order to convert the IMFP to an attenuation length, the equation of Seah and Spencer [5] can be used. For materials commonly encountered in semiconductor fabrication the value of λ falls within the range 1.5–3.5 nm.

The expression for the XPS signal that is emitted from the surface of a thin film can be shown to be

$$I = I_0 [1 - \exp(-d/\lambda \cos \theta)] \quad (2)$$

Eqs. (1) and (2) form the basis of the analysis method employed for this work.

The way in which these equations can be manipulated so that the thickness of each layer of a multi-layer sample has been described elsewhere [6,7].

These methods apply to thin layers of material that are continuous and uniform over the whole of the analysis area. They should not be applied in their simple form if the layers are discontinuous.

In this paper a method will be described whereby partial coverage of a thin layer can be detected and an estimate given of the fraction of the substrate that is covered by the thin layer. The method will then be applied to XPS data from three sets of HfO_2 layers grown on silicon using atomic layer deposition (ALD). For each set of samples, the silicon surface had received a different surface treatment prior to the growth of the layers.

The results obtained by XPS will be compared with those from ToF SIMS. Rutherford backscattering (RBS) was used to provide an absolute value for the quantity of HfO_2 per unit area of the film.

HfO_2 is a candidate material for the replacement of silicon dioxide as the gate dielectric material in future transistors. For this application, it is essential that the dielectric forms continuous, uniform layers on silicon or silicon dioxide. Using ARXPS it should be possible to determine whether the layer is continuous and uniform or whether only partial coverage of the silicon has been achieved.

2. Experimental

2.1. ARXPS

The ARXPS measurements were made using a Theta Probe XPS instrument from Thermo Electron. This instrument uses a focused, monochromated X-ray beam. Al $K\alpha$ radiation was used throughout the work (photon energy 1486.6 eV). For this work, an X-ray spot size of 400 μm was used.

Theta Probe uses a method of parallel ARXPS measurements. This means that the sample remains in at a single position throughout the measurement and is not tilted. A two-dimensional detector is positioned at the exit of a hemispherical electron energy analyser. The photoelectrons are dispersed according to their kinetic energy along one axis of a two-dimensional detector and according to their emission angle along the other axis. The instrument collects photoelectrons emitted over an angular range of 23–83°. The detector has 112

channels and so the angular range can be uniformly distributed amongst these channels. In order to achieve the optimum compromise between angular resolution and acquisition time, these channels were combined in such a way that 16 angular channels were measured with each channel having an angular range of 3.75°.

2.2. TOF-SIMS

TOF-SIMS data were collected using an Iontof IV instrument, with a Ga^+ primary ion beam at 15 keV. All measurements were performed in static mode with ion doses not exceeding $1\text{E}12$ ions/ cm^2 . The Si^+ and Hf^+ intensities were used in this study in order to investigate the closure of the film.

2.3. RBS

RBS results were acquired on a RBS-400 endstation installed around a 2 MV 6SDH-1 Pelletron accelerator. The beam energy was 1 MeV while the scatter angle was 168°. The solid angle of the detector was 0.6 mSr. Due to the high scattering cross-section of Hf, a dose of 20 μC was sufficient to obtain detection limits down to 10^{14} Hf/ cm^2 . Areal density was calculated with the RUMP analysis program.

2.4. Silicon surface preparation

Three different starting surfaces were evaluated in this work: a thin thermal oxide grown at 650°C in a RTO (rapid thermal oxidation) process, representing a low OH concentration surface, a chemical oxide grown using ozonated chemistries, representing a high OH concentration surface and a H-terminated surface (HF-dip Si). These surfaces were shown to have different growth characteristics regarding the growth of HfO_2 films [8].

2.5. ALD high- k layer growth

All layers studied in this work were grown in a Pulsar 8200 ALCVDTM ASM reactor. All layers were grown at 300 °C using $\text{Al}(\text{CH}_3)_3$ and HfCl_4 as metal reactant for Al_2O_3 and HfO_2 layers respectively. The oxidizing reactant was H_2O in both cases. The ALCVD process consist of alternating, self-limiting reaction of each reactant separated by a N_2 purge in order to avoid direct reaction of the two reactants in the gas phase and the process is described by the number of cycles (metal-purge-water-purge) needed to grow the layer.

3. The model

Fig. 1 illustrates the model used in the calculations described here, in this case Al_2O_3 grown on a layer of SiO_2 on silicon has been used as an illustration. For this model, it is assumed that the layer of SiO_2 , of thickness d_s , is uniform and thin enough for the XPS signal from the silicon substrate to be observed. The Si 2p signal is used in the calculations involving both the elemental silicon and the oxidised silicon. The difference in kinetic energy between the photoelectrons emitted from the

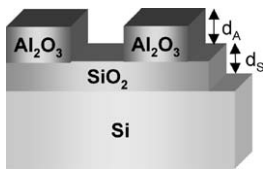


Fig. 1. The model used to calculate the fractional coverage of material.

elemental silicon and those from the oxidised silicon is very small and it can be assumed that the signals are attenuated equally by the aluminium oxide at the surface.

The layer of Al_2O_3 is assumed to have grown in a non-uniform manner, producing island structures on the silicon dioxide. The thickness of the islands is d_A and the fractional coverage is f ($0 \leq f \leq 1$). It must be assumed that the islands of Al_2O_3 and the spaces between the islands are such that shadowing of the signal emitted from the uncovered SiO_2 is not significant. For this work, the signal from Al 2p was measured.

This model uses the ratio of peak areas for the Al 2p and the Si 2p from the SiO_2 . The way in which this ratio varies with angle is dependent upon both the thickness of the layers and the fractional coverage of Al_2O_3 .

The Al 2p signal from Al_2O_3 is given by

$$I_A = fI_{A,0} \cos(\theta) [1 - \exp(-d_A/\lambda_{A,A} \cos(\theta))]$$

where $I_{A,0}$ is the signal from a thick layer of Al_2O_3 , $\lambda_{A,A}$ the attenuation length of the Al 2p photoelectron in the Al_2O_3 layer, d_A the thickness of the dielectric islands (see Fig. 1).

The Si 2p signal from the SiO_2 layer is composed of two parts; one that reaches the detector without passing through the Al_2O_3 layer ($I_{S,U}$) and one that is attenuated by passing through the Al_2O_3 layer ($I_{S,A}$). These are given by

$$I_{S,U} = \{1 - f\} \{I_{S,0} \cos(\theta) [1 - \exp(-d_S/\lambda_{S,S} \cos(\theta))]\}$$

$$I_{S,A} = \{f\} \{I_{S,0} \cos(\theta) [1 - \exp(-d_S/\lambda_{S,S} \cos(\theta))] \times [\exp(-d_A/\lambda_{S,A} \cos(\theta))]\}$$

where $I_{S,0}$ is the signal from a thick layer of SiO_2 , $\lambda_{S,S}$ the attenuation length of a Si 2p electron in SiO_2 , $\lambda_{S,A}$ the attenuation length of a Si 2p electron in Al_2O_3 , d_S the thickness of the SiO_2 layer (see Fig. 1).

The total Si 2p signal is then given by

$$I_{S,T} = I_{S,U} + I_{S,A}$$

It is now possible to compute the ratio $I_A/I_{S,T}$ which is the ratio of the Al 2p signal to the Si 2p (oxide) signal as a function of both angle and fractional coverage. As an example, Fig. 2 shows a set of curves computed for a 1 nm layer of SiO_2 having a 1 nm layer of Al_2O_3 grown on it with a fractional coverage in the range 0.2–1. As can be seen, the curves are very sensitive to coverage, especially at large angles. Note that the ordinate in Fig. 2 is a logarithmic scale because of the very large data range.

At a constant fractional coverage of Al_2O_3 , the sensitivity of the curves to the thickness, d_A , is illustrated in Fig. 3. In this illustration, the coverage, f , is 0.7.

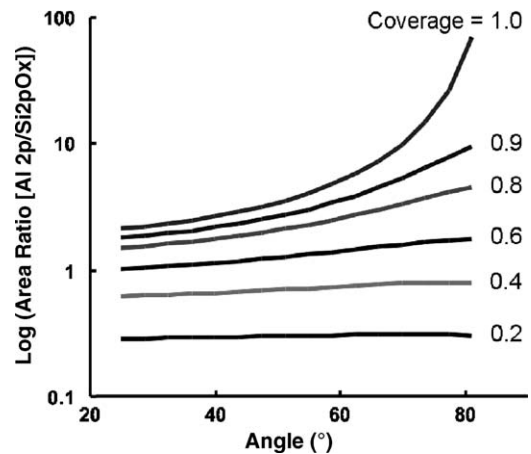


Fig. 2. The calculated ratio of the Al 2p peak area to that of Si 2p (oxidised) as a function of angle for Al_2O_3 grown on 1 nm of SiO_2 on Si. Curves are shown for a thickness of Al_2O_3 (d_A) of 1 nm and a range of coverage (f) from 0.2 to 1.

Fig. 4 illustrates how the curves change with coverage of Al_2O_3 when the total quantity of the material is fixed. Curves are shown for $f = 1$, $d_A = 1$ nm; $f = 0.5$, $d_A = 2$ nm and $f = 0.25$, $d_A = 4$ nm. Again, the ordinate is expressed in a logarithmic scale to accommodate the range of the data.

These curves serve to illustrate the sensitivity of the model to changes in the structure of the material. In order to use this model in practice, the thickness of the SiO_2 layer must be measured first. This can be done on each wafer using ARXPS data from the oxidised and elemental Si 2p XPS signal. This is accomplished in the normal way, using the equation:

$$\ln[1 + R/R_0] = d_S/(\lambda_{S,S} \cos \theta)$$

In this case, R is the experimentally measured peak area ratio for the Si 2p peak from oxidised and elemental silicon. R_0 is the same peak intensity ratio but from thick (>100 nm) layers of silicon dioxide and silicon. The value of R_0 (0.933) used in this work is that reported by Seah and Spencer [5]. If the expression on the left hand side of the equation is plotted against $1/\cos \theta$ then the gradient is $d_S/\lambda_{S,S}$ and the thickness of the layer can be calculated easily if $\lambda_{S,S}$ is known. It is

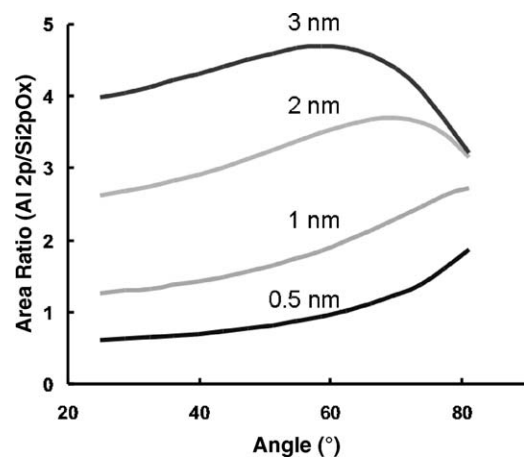


Fig. 3. The calculated ratio of the Al 2p peak area to that of Si 2p (oxidised) as a function of angle for Al_2O_3 grown on 1 nm of SiO_2 on silicon. Curves are shown for a fractional coverage (f) of 0.7 and thickness (d_A) in the range 0.5–3 nm.

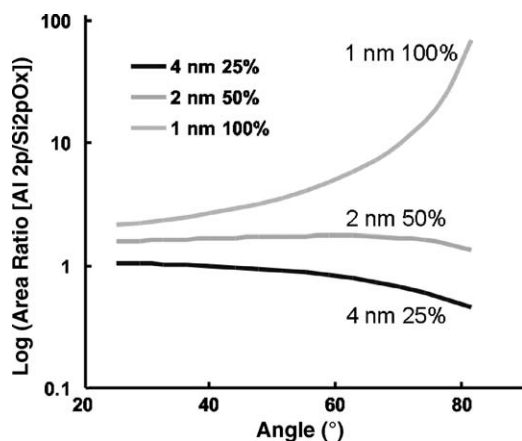


Fig. 4. The calculated ratio of the Al 2p peak area to that of Si 2p (oxidised) as a function of angle for Al_2O_3 grown on 1 nm of SiO_2 on Si. Curves are shown for a constant quantity of material.

important in measurements of this nature to avoid the complications associated with elastic scattering in the sample. In practice, this means avoiding the use of data from angles greater than 60° .

For the next step, the value for d_s can then be inserted into the equation for $I_A/I_{S,T}$. Using least squares fitting, the experimental Al 2p/Si 2p (oxidised) peak intensity ratio can be fitted to the equation using d_A and f as fitting parameters. For this measurement the whole of the angular range was used in order to provide the maximum precision in the coverage determination. For this type of calculation, the effects of elastic scattering at the large angles are thought to be small because the layers from which the XPS signals are derived are very thin.

This procedure was applied to a sample having a SiO_2 layer of 0.8 nm, determined using ARXPS and a layer of Al_2O_3 grown using five ALD cycles, Fig. 5. The experimental data (solid squares) are shown superimposed upon a set of curves equivalent to those shown in Fig. 2. The best fit to the data was achieved for a value of $f = 0.49$.

The procedure was applied to a set of similar samples each having been prepared using a different number of

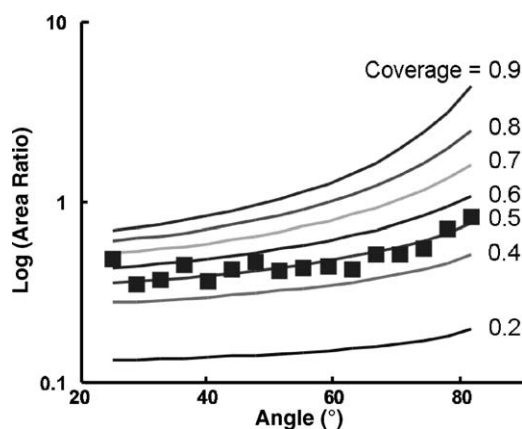


Fig. 5. Experimental Al 2p/Si 2p (oxidised) peak intensity ratios compared with a set of curves showing the expected ratios. The best fit was achieved at a fractional coverage of 0.49.

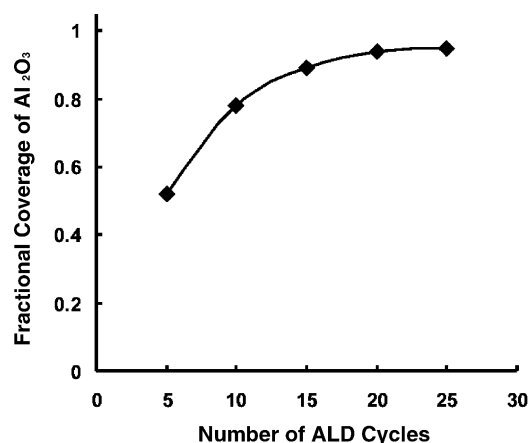


Fig. 6. Coverage of Al_2O_3 as a function of the number of ALD cycles.

ALD cycles. Fig. 6 shows the way in which the fractional coverage changes as a function of the number of cycles. complete coverage is only observed after about 20 ALD cycles.

As a test of this model, when the fractional coverage reaches unity then the thickness of the Al_2O_3 calculated using the model should be the same as the thickness calculated using the more conventional ARXPS techniques [6,7]. Fig. 7 shows the ratio of the measured thickness using each method as a function of the number of ALD cycles used to produce the layer.

The curve shown on this figure is a simple exponential decay function fitted to the data. The optimum fit is achieved with an asymptote at 0.99. This suggests that the model is consistent with measurements of overlayer thickness using the models based on continuous overlayers.

A result such as this can only be achieved if the model is correct and if the overlayers are uniform. A value differing significantly from unity might suggest that the overlayer, although continuous, does not have a uniform thickness or the SiO_2 layer thickness is not uniform.

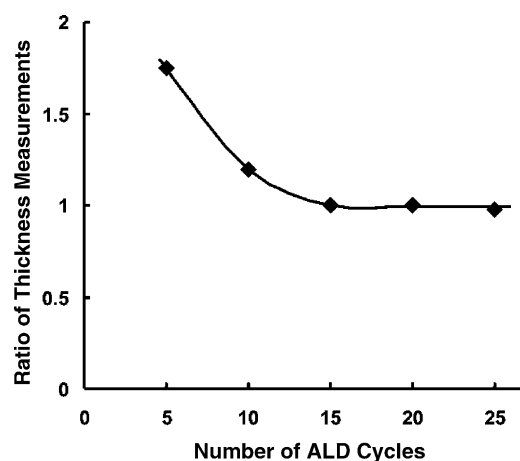


Fig. 7. Ratio of the thickness calculated using the model described here to that calculated from a model that assumes complete coverage of uniform layers.

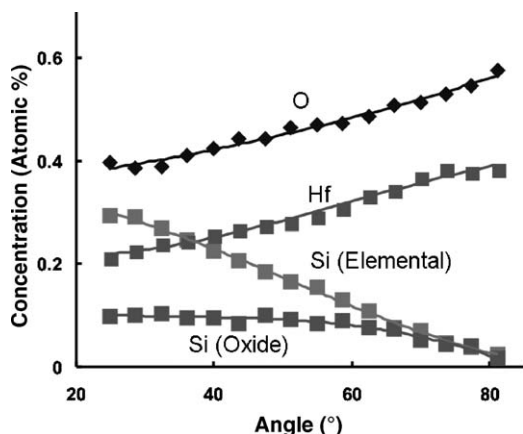


Fig. 8. Normalised ARXPS signal as a function of emission angle from a layer of HfO_2 on thermally grown SiO_2 on silicon. In this example, the HfO_2 was grown using 20 ALD cycles.

4. Results

4.1. Fractional coverage of HfO_2

ARXPS data was collected from each wafer in each of the three wafer sets. Following acquisition of the data, the peak areas were measured. The relative sensitivity factors were applied along with the corrections for instrument transmission function. A typical data set is shown in Fig. 8, here the data has been normalised at each angle to produce curves of atomic concentration versus angle. The data set shown here is from a silicon wafer having 0.95 nm of thermally grown SiO_2 on its surface followed by 20 ALD cycles of HfO_2 . From this information, the required ratio of the signals can be measured ($\text{Hf } 4f/\text{Si } 2p$ (oxide)) as a function of angle (equivalent to the data shown as solid squares in Fig. 5).

This procedure was performed on all of the wafers and the fractional coverage calculated in the manner described above.

The way in which the coverage of HfO_2 varies with the number of ALD cycles for growth on each type of surface is shown in Fig. 9.

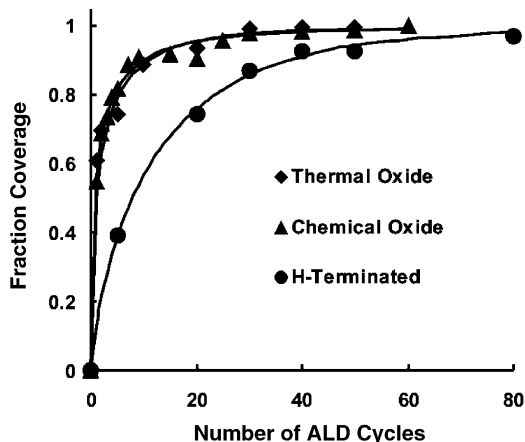


Fig. 9. The fractional coverage of HfO_2 , determined by ARXPS, as a function of the number of ALD cycles for dielectric growth on each of the three types of surface.

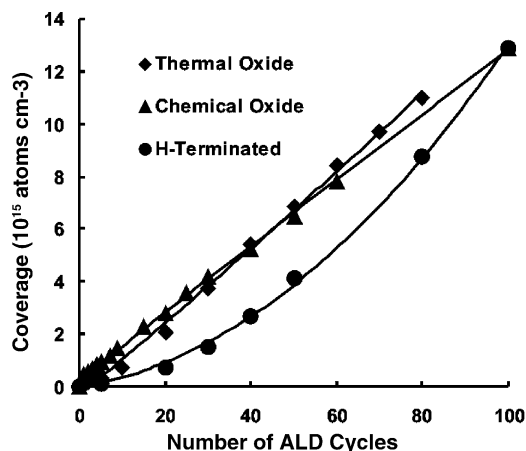


Fig. 10. The coverage of HfO_2 , as determined by RBS, as a function of the number of ALD cycles for each of the three types of surface.

From Fig. 9, it appears that the relationship between the fractional coverage attained as a function of the number of ALD cycles is very similar on thermal oxide and chemical oxide surfaces. A larger number of ALD cycles is required on an H-terminated surface in order to achieve the same fractional coverage.

The quantity of HfO_2 on these surfaces has been determined using RBS and the results are shown in Fig. 10. This indicates that the growth rate per ALD cycle is influenced by the nature of the initial surface. The data shown in Fig. 9 can be converted using the data in Fig. 10 to show the fractional coverage of HfO_2 as a function of the quantity of material per unit area. This is shown in Fig. 11.

It can be seen from this figure that, for a given loading of the dielectric material, the fraction of the surface covered by HfO_2 depends upon the nature of the initial surface. The growth on the thermal oxide leads to the greatest coverage while growth on the H-terminated surface leads to the smallest coverage.

4.2. Comparison of methods

The ratio of the HfO_2 thickness calculated using this method and that calculated by the traditional ARXPS methods is shown

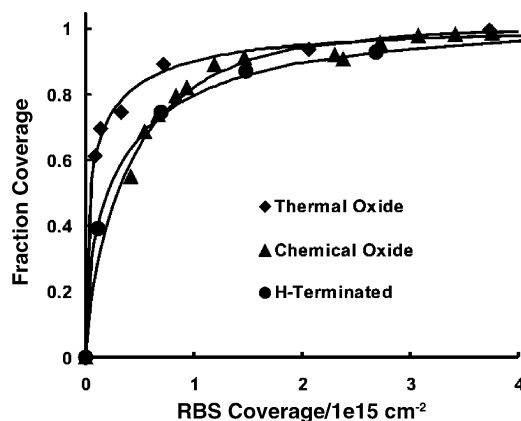


Fig. 11. The fractional coverage of HfO_2 , determined by ARXPS, as a function of the number of the coverage determined using RBS for dielectric growth on each of the three types of surface.

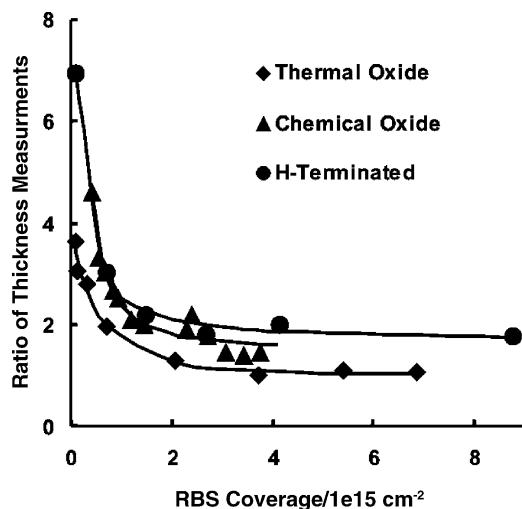


Fig. 12. Ratio of the thickness calculated using the model described here to that calculated from a model that assumes complete coverage of uniform layers for each set of wafers.

in Fig. 12 as a function of HfO_2 coverage for each set of wafers. As with the Al_2O_3 layers the ratio is asymptotic to unity for layers grown on the thermal oxide but the asymptote is greater than unity for the other two types of surface. This suggests that, even when the fractional coverage reaches unity, there is non-uniformity within the layers grown on the thermal oxide and the H-terminated surface.

4.3. Comparison with SIMS

Static SIMS spectra were collected from the three sets of wafers. The intensity of the $^{30}\text{Si}^+$ peak, relative to its intensity when no HfO_2 was present, provides some indication of the coverage of the surface. Fig. 13 shows how this relative intensity varies with the quantity of HfO_2 on the wafer, as determined by RBS.

This figure is consistent with the data shown in Fig. 11. It suggests that, on the thermal oxide and the chemical oxide surface, complete coverage is achieved at smaller loadings of HfO_2 than is the case with the H-terminated surface.

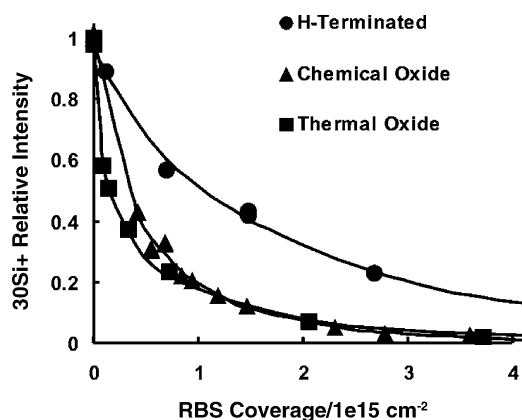


Fig. 13. The relative intensity of the $^{30}\text{Si}^+$ peak in the SIMS spectrum as a function of the coverage of HfO_2 .

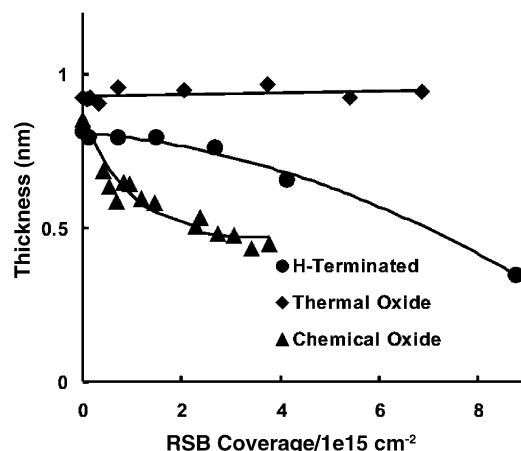


Fig. 14. The thickness of the silicon dioxide layer as a function of the coverage of HfO_2 .

4.4. The silicon dioxide layer

The ARXPS data was also used to measure the thickness of the SiO_2 intermediate layer on each wafer. The results are shown in Fig. 14.

The SiO_2 thickness was found to be independent of the HfO_2 coverage on the wafers having the thermally grown oxide. On the H-terminated and chemical oxide surfaces, the SiO_2 was found to be thinner on those wafers having a greater coverage of HfO_2 . This behaviour may indicate that the SiO_2 layer increases in thickness when exposed to air when the HfO_2 layer is incomplete.

The chemical state of the silicon was also found to depend upon the coverage of HfO_2 and the nature of the original surface. As an example, Fig. 15 shows a comparison of the Si 2p region of the XPS spectrum from two of the wafers. These were both from the wafers that were H-terminated, one had no HfO_2 grown on the surface while the other had 50 ALD cycles grown (4.14×10^{15} atoms/cm²). To improve clarity in this figure, a Shirley background has been subtracted from each spectrum, the contribution of the Si $2p_{3/2}$ signal has been subtracted and the intensity of the two spectra normalised for the signal from oxidized silicon. Note that the original H-terminated surface would have very little oxidized silicon but exposure to air has caused the growth of the native oxide.

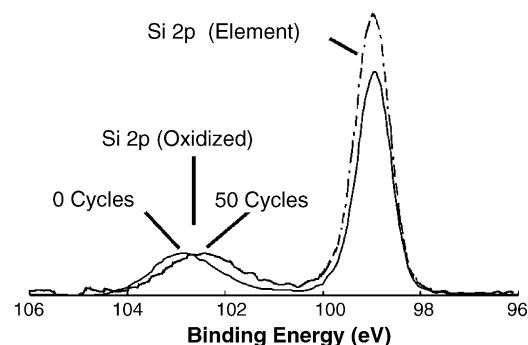


Fig. 15. The silicon $2p_{3/2}$ XPS spectrum from H-terminated wafers having no HfO_2 growth and 50 ALD cycles grown on it.

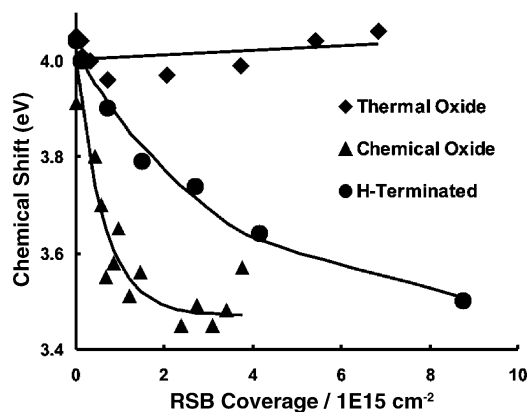


Fig. 16. The dependence of the chemical shift of oxidized Si 2p upon the number of ALD cycles for each of the three types of wafer.

The difference in the binding energy for the oxidised Si between the two wafers is approximately 0.5 eV, suggesting that there may be silicate formation.

Fig. 16 shows the chemical shift of the oxidised silicon relative to the elemental silicon for all of the wafers measured in this study.

For the thermal oxide, there is little dependence of the chemical shift upon the number of ALD cycles. The chemical shift is close to 4 eV, suggesting that the oxidized silicon is present as SiO₂. For the other two types of wafer, the chemical shift is close to 3.5 eV at high coverage of HfO₂ suggesting silicate formation [6,9]. The initial rate of change of chemical shift with coverage is much greater with the chemical oxide surface than with the H-terminated surface.

5. Discussion

The model described above is capable of providing an estimate of the fractional coverage of a surface with a thin layer of material. The model assumes that when coverage is incomplete the thickness of the “islands” of material present is uniform. This is unlikely to be the case and may be a cause of error in the absolute value for the fractional coverage reported. However, the model appears to be unambiguous in its indication that coverage is incomplete and useful in comparing one wafer with another. The model can provide a good indication of the loading of material required to produce a continuous overlayer. It shows trends in the behaviour of the HfO₂ layers on the three types of surface studied here. Growth on thermal oxide provides better coverage and uniformity than growth on the chemical oxide, which in turn, provides better coverage and uniformity than layers grown on an H-terminated surface.

The model is consistent with the one described in reference [6], which can be used for continuous, uniform layers. The data here also suggests that the model can be used to indicate whether the overlayer thickness is uniform.

RBS would report a coverage of about 9×10^{14} atoms cm⁻² for a complete, uniform monolayer of HfO₂ on SiO₂. This means that if the loading is below this value, however uniform the layer, there cannot be complete coverage. The data reported here are consistent with this. The layers grown on the thermal oxides show the highest coverage at a given loading and appear to be the most uniform. Nevertheless, the model always indicates fractional coverage when the loading of HfO₂ is less than 9×10^{14} atoms cm⁻².

The behaviour of the silicon dioxide layer deserves comment. It appears that the thermal oxide is stable. Its thickness does not change with time even when the coverage of HfO₂ is incomplete. On the other two surfaces, the SiO₂ layer appears to grow after the growth of the HfO₂ has taken place. This is presumably due to the action of atmospheric oxygen or water on the thin SiO₂ layers. If there is sufficient HfO₂ on the surface to provide complete surface coverage, this may prevent further growth of SiO₂. It is not clear from this work whether further growth occurs only in the spaces between the islands of HfO₂ or whether diffusion of oxygen through the islands is also occurring. This behaviour may account, in part, for the fact that the asymptotes in Fig. 12 are not all at unity.

XPS can distinguish between silicon oxide and silicate and this work shows that, at high coverage, silicate is formed if the initial surface is either H-terminated or chemical oxide. Only silicon dioxide is present when HfO₂ is grown on the thermal oxide. If coverage is incomplete, exposure to air causes a change to the nature of the oxidised silicon such that it becomes more like SiO₂.

References

- [1] T. Conard, W. Vandervorst, J. Petry, C. Zhao, W. Besling, H. Nohira, O. Richard, *Appl. Surf. Sci.* 400 (2003) 203–204.
- [2] M.P. Seah, et al. *Surf. Interface Anal.* 36 (2004) 1269.
- [3] S. Tanuma, C.J. Powell, D.R. Penn, *Surf. Interface Anal.* 21 (1994) 165.
- [4] NIST Electron Effective Attenuation Length Database, Prepared by C.J. Powell, A. Jablonsci, NIST Standard Reference Database 82.
- [5] M.P. Seah, S.J. Spencer, *Surf. Interface Anal.* 33 (2003) 515–524.
- [6] R. Champanaria, P. Mack, R. White, J. Wolstenholme, *Surf. Interface Anal.* 35 (2003) 1028.
- [7] R.G. Vitchev, J.J. Pireaux, T. Conard, H. Bender, J. Wolstenholme, *Chr. Defranoux, Appl. Surf. Sci.* 235 (2004) 21–25.
- [8] M.L. Green, M.-Y. Ho, B. Busch, G.D. Wilk, T. Sorsch, T. Conard, B. Brijs, W. Vandervorst, P.I. Raisen, D. Muller, M. Bude, J. Grazul, *J. Appl. Phys.* 92 (2002) 7168.
- [9] P. Panchaipetch, G. Pant, M. Quevedo-Lopez, H. Zhang, M. El-Bouanani, M.J. Kim, R.M. Wallace, B.E. Gnade, *Thin Solid Films* 68 (2003) 425.